




Evaluating drivers of spatiotemporal variability in individual condition of a bottom-associated marine fish, Atlantic cod (*Gadus morhua*)

M. Lindmark ^{1,*}, S. C. Anderson^{2,3}, M. Gogina ⁴, and M. Casini ^{1,5}

¹Department of Aquatic Resources, Swedish University of Agricultural Sciences, Institute of Marine Research, Turistgatan 5, 453 30 Lysekil, Sweden

²Pacific Biological Station, Fisheries and Oceans Canada, Nanaimo, V9T 6N7 BC, Canada

³Department of Mathematics, Simon Fraser University, Burnaby, V5A 1S6 BC, Canada

⁴Leibniz Institute for Baltic Sea Research, Seestraße 15, 18119 Rostock, Germany

⁵Department of Biological, Geological and Environmental Sciences, University of Bologna, Via Selmi 3, 40126 Bologna, Italy

* Corresponding author: tel: +46(0)104784137; e-mail: max.lindmark@slu.se.

An organism's body condition describes its mass given its length and is often positively associated with fitness. The condition of Atlantic cod (*Gadus morhua*) in the Baltic Sea has declined dramatically since the early 1990s, possibly due to increased competition for food and hypoxia. However, the effects of biotic and abiotic variables on body condition have not been evaluated at local scales, which is important given spatial heterogeneity. We evaluate changes in distribution, experienced environmental conditions, and individual-level condition of cod in relation to covariates at different spatial scales using geostatistical models with spatial and spatiotemporal random effects. Sprat, *Saduria entomon*, temperature and oxygen were positively associated with condition, and depth was negatively associated. However, the effects of explanatory variables were small—spatial and spatiotemporal latent variables explained 5.7 times more variation than all covariates together (year excluded). Weighting environmental oxygen with local biomass densities revealed steeper declining trends compared to the unweighted oxygen in the environment, while the effect of weighting was less clear for condition. Understanding the drivers of spatiotemporal variation in body condition is critical for predicting responses to environmental change and to effective fishery management; yet low explanatory power of covariates on individual condition constitutes a major challenge.

Keywords: density dependence, deoxygenation, Le Cren's condition factor, spatial analysis, spatio-temporal models, species distribution models.

Introduction

Body condition is a morphometric index that describes the “plumpness” of an organism, or its weight relative to its length (Nash *et al.*, 2006; Lloret *et al.*, 2014). It is related to food intake rates and metabolic activity and is often positively associated with fitness (Bolger and Connolly, 1989; Morgan *et al.*, 2010). In fishes, individuals with high condition have greater reproductive potential and success (Hislop *et al.*, 1978; Marshall and Frank, 1999), and poor condition increases the likelihood of skipped spawning (Jørgensen *et al.*, 2006; Mion *et al.*, 2018) and can lower chances of survival (Dutil and Lambert, 2000; Casini *et al.*, 2016b). Hence, body condition constitutes a valuable index for evaluating changes in productivity of fish stocks from ecosystem changes (Thorson, 2015; Grüss *et al.*, 2020).

Because of the link to food consumption, interannual variation in condition is often associated with changes in the strength of competition for food, via changes in density of the population, competitors, or prey species (Cardinale and Arrhenius, 2000; Casini *et al.*, 2006; Thorson, 2015; Grüss *et al.*, 2020). Condition has also been linked to abiotic environmental variables (e.g. temperature and salinity) affecting ecosystem productivity and local habitat quality (Möllmann *et al.*, 2003; Morgan *et al.*, 2010; Thorson, 2015; Grüss *et al.*, 2020). More recently, studies have found a link between

declining body condition and deoxygenation (often resulting in the expansion of “dead zones” causing habitat degradation and compression) (Casini *et al.*, 2016a, 2021), fueled by warming and nutrient enrichment (Diaz, 2001; Breitburg, 2002; Diaz and Rosenberg, 2008; Carstensen *et al.*, 2014). Moreover, laboratory experiments have shown that warming is associated with lower condition unless fish have food in excess (Cui and Wootton, 1988). This suggests effects of deoxygenation and warming could be synergistic, as reduced oxygen concentrations also cause lower food intake rates, even during milder hypoxia (Chabot and Dutil, 1999). As both environmental and biological variables can affect condition, it is important to study their relative contribution to condition in a common framework.

The Baltic Sea constitutes an interesting case study for disentangling ecosystem drivers affecting body condition (Reusch *et al.*, 2018). First, in the eastern Baltic Sea cod stock (hereafter referred to as cod), the average body growth and body condition have declined since the collapse of the stock in the early 1990s (Casini *et al.*, 2016a; Mion *et al.*, 2021). This has compromised the stock's productivity to the extent that population biomass is expected to remain below safe limits despite the ban of targeted cod fisheries in 2019 (ICES, 2021a, 2021b). Second, the Baltic Sea ecosystem has seen a major change in the abundance and distribution of both cod

Received: 21 October 2022; Revised: 29 March 2023; Accepted: 1 May 2023

© The Author(s) 2023. Published by Oxford University Press on behalf of International Council for the Exploration of the Sea. This is an Open Access article distributed under the terms of the Creative Commons Attribution License (<https://creativecommons.org/licenses/by/4.0/>), which permits unrestricted reuse, distribution, and reproduction in any medium, provided the original work is properly cited.

and its potential competitors for the benthic prey *Saduria entomon* (Haase *et al.*, 2020; Neuenfeldt *et al.*, 2020)—the flounder species complex (European flounder *Platichthys flesus* and Baltic Flounder *Platichthys solemdali*) (Orio *et al.*, 2017) and the main pelagic prey of cod (sprat *Sprattus sprattus* and herring *Clupea harengus*) (Casini *et al.*, 2011; Eero *et al.*, 2012; ICES, 2021a). Also increased intraspecific competition has been linked to the low growth rates of the stock (Svedäng and Hornborg, 2014). Lastly, the irregular inflows of saline and oxygenated water from the North Sea together combined with a slow water exchange (a residence time of 25–30 years) are features that have contributed to making the Baltic Sea the largest anthropogenically induced hypoxic area in the world (Carstensen *et al.*, 2014). It is also one of the fastest warming regional seas (Belkin, 2009; Reusch *et al.*, 2018). Previous studies have linked changes in mean condition of cod over large spatial scales to single or some combination of ecosystem drivers (Casini *et al.*, 2016a, 2021; Orio *et al.*, 2020). However, in previous studies, within-population variability in condition has been neglected, and the effects of environmental and biotic covariates have not been studied on local scales. Moreover, the effect of all the above-mentioned covariates on cod condition has not been analysed in a common framework.

In this study, we apply geostatistical models to characterize the spatiotemporal variation in individual-level body condition and distribution of cod in the south-eastern Baltic Sea. We use data from scientific surveys between 1993 and 2019, which corresponds to a period of initially high but then deteriorating cod condition (Casini *et al.*, 2016a). We then address three aims: (1) identify which covariates [biomass densities of flounder and cod (representing competition), *S. entomon* (benthic prey), biomass of sprat and herring (pelagic prey), as well as depth, oxygen concentration and temperature], at different spatial scales (from haul-location to ices rectangle and for pelagic fishes, also basin-level), can explain observed variation in condition; (2) develop a spatiotemporally standardized, biomass-weighted condition index for cod that takes into account the heterogeneous and temporally varying distribution of cod; and (3) explore how the spatiotemporal distribution of cod impacts the environmental conditions experienced and the implications of it for body condition trends.

Materials and methods

Data

To model the spatiotemporal development of cod condition and distribution, we acquired weight and length data for 94295 individual cod, as well as catch per unit effort data (CPUE, numbers/hour) of cod by 10-mm length class from the Baltic International Trawl Survey (BITS) between the years 1993 and 2019 in the International Council for the Exploration of the Sea (ICES) subdivisions 24–28 (*SI Appendix*, Figure S1). CPUE data were standardized based on gear dimensions and towing speed (TVL trawl with 75 m sweeps at 3 knots) to catch per swept area of 0.45 km², following Orio *et al.* (2017), which we then expressed in units kg/km². Abundance density was converted to biomass density by fitting annual weight-length regressions (*SI Appendix*, Figure S2). We used only data from the fourth quarter (mid-October to mid-December), which corresponds to the main growing and feeding season of cod (Aro, 1989) and also the quarter

in which the Baltic International Acoustic Survey (BIAS) is conducted, meaning sprat and herring biomass can be used as covariates. The BITS data can be downloaded from <https://www.ices.dk/data/data-portals/Pages/DATRAS.aspx>.

Estimating spatiotemporal development of body condition and biomass density

Condition model

We modelled cod condition using a spatiotemporal version of Le Cren's relative condition factor (K_{rel}) (note we reserve the term “condition index” for the annual, model-based index, see *Spatiotemporal predictions* below). This factor is defined as the ratio between the observed weight for individual fish i , caught in time t at space s , and the predicted weight. The predicted weight was given by the relationship $\bar{w} = a l^b$, where parameters a and b were estimated in a non-spatial model with all years pooled, to represent the average weight prediction, \bar{w} based on observed lengths l . An individual cod with a $K_{rel} = 1$ thus has the average condition across years and space in the domain. Unlike Fulton's K , Le Cren's relative condition factor does not rely on the assumption that growth is isometric ($b = 3$), which, if violated, leads to bias when comparing condition of different lengths as the condition factor scales in proportion to l^{b-3} (Le Cren, 1951). Spatially correlated residual variation was accounted for with spatial random effects through Gaussian random fields. This approach to modelling spatiotemporal data is an increasingly popular method for explicitly accounting for spatial and spatiotemporal variation due to its ability to improve predictions of fish density (Thorson *et al.*, 2015a) and range shifts (Thorson *et al.*, 2015b) and its availability in open source software such as the R package “INLA” (Rue *et al.*, 2009; Lindgren *et al.*, 2011).

To assess the ability of covariates (see the section *Covariates*) to explain variation in condition, we fit a geostatistical generalized linear mixed-effects model (GLMM) to the natural log of the Le Cren condition factor (in location s and time t), assuming Student- t distributed residuals with the degrees of freedom parameter (ν) set to 5 due to the presence of extreme values:

$$\log(K_{rel}) \sim \text{Student-}t(\mu_{s,t}, \phi, \nu), \quad (1)$$

$$\mu_{s,t} = \mathbf{X}_{s,t} \boldsymbol{\beta} + \omega_s + \epsilon_{s,t}, \quad (2)$$

$$\omega \sim \text{MVNormal}(0, \boldsymbol{\Sigma}_\omega), \quad (3)$$

$$\epsilon_t \sim \text{MVNormal}(0, \boldsymbol{\Sigma}_\epsilon), \quad (4)$$

where K_{rel} represents the Le Cren condition factor at space s (a vector of two UTM zone 33 coordinates) and time t , μ represents the mean weight, and ϕ represents the scale parameter. $\mathbf{X}_{s,t}$ is the design matrix, with the following covariates: year (as a factor), biomass densities of flounder and cod, biomass of sprat, herring and *S. entomon*, depth, oxygen concentration, and temperature) at different scales (from local to large scale), and $\boldsymbol{\beta}$ is a vector of fixed effect coefficients. The parameters ω_s and $\epsilon_{s,t}$ (Equations 3–4) represent spatial and spatiotemporal random effects, respectively. Spatial and spatiotemporal random effects were assumed to be drawn from Gaussian random fields (Lindgren *et al.*, 2011; Cressie and Wikle, 2011) with covariance matrices $\boldsymbol{\Sigma}_\omega$ and $\boldsymbol{\Sigma}_\epsilon$. We chose to model the spatiotemporal random fields as independent for each year given the correlation when estimated as first-order autoregressive

was near zero and had confidence intervals overlapping 0. The covariance ($\Phi(s_j, s_k)$) between spatial points s_j and s_k in all random fields is given by a Matérn function.

Density models

We fit spatiotemporal GLMMs to biomass density data in a similar fashion as for condition to (1) use predicted local densities of cod and flounder as covariates in the condition model, (2) acquire local biomass weights to weight the spatiotemporal predictions of condition with local biomass density when calculating the annual condition index (see the section *Spatiotemporal predictions*), and (3) evaluate how the depth distribution of cod, as well as oxygen and temperature conditions experienced by cod, have changed. For the third task, we used the predicted density at space s and time t as weights when calculating the annual median (and interquartile range) depth, oxygen concentration, and temperature.

We modelled densities using a Tweedie distribution with a log link function, as density is positive, continuous, and contains zeros (Tweedie, 1984; Shono, 2008; Anderson *et al.*, 2019):

$$y_{s,t} \sim \text{Tweedie}(\mu_{s,t}, p, \phi), \quad 1 < p < 2, \quad (5)$$

$$\mu_{s,t} = \exp(\mathbf{X}_{s,t}\boldsymbol{\beta} + \omega_s + \delta_{s,t}), \quad (6)$$

$$\delta_t = 1 \sim \text{MVNormal}(0, \boldsymbol{\Sigma}_\epsilon), \quad (7)$$

$$\delta_{t>1} = \rho\delta_{t-1} + \sqrt{1 - \rho^2}\epsilon_t, \quad \epsilon_t \sim \text{MVNormal}(0, \boldsymbol{\Sigma}_\epsilon), \quad (8)$$

where $y_{s,t}$ represents density (kg/km²) at space s and time t , μ is the mean density, and p and ϕ represent power and dispersion parameters, respectively. We use year as a factor, and the remaining covariates (see the section *Covariates*) were modelled with smooth functions, implemented as penalized splines. The parameters ω_s have the same definition as in the condition model (Equation 3), but the spatiotemporal random effects are here assumed to follow a stationary AR1-process where ρ represents the correlation between subsequent spatiotemporal random fields.

Covariates

For both models (condition and density), covariates were chosen to reflect hypothesized drivers based on published literature. For the condition model, we included covariates at spatial scales that roughly reflect the habitats cod would have been exposed to during the seasonal build-up of energy reserves. Recent tagging studies suggest cod are either stationary or mobile over the course of a year moving between feeding and spawning habitats (Mion *et al.*, 2022). However, within the feeding season, stationary cod move roughly over an area corresponding to an ICES rectangle (1 × 0.5 degree cells, *SI Appendix*, Figure S1) (Hüssy *et al.*, 2020). Recent tagging studies, however, show that some cod are more mobile throughout the year (Hüssy *et al.*, 2020). Therefore, we included environmental and biological covariates [sea bottom temperature (°C), sea bottom oxygen (ml/l), depth (m), and biomass density of *S. entomon* (mg/m²), cod and flounder (kg/km²)] at the haul level and the median over the ICES rectangle-level. We also explored the effect of lagging oxygen and temperature covariates at the ICES rectangle-level with 1 quarter (which was not possible for biotic data), to reflect that these large-scale variables are introduced to capture past exposure affecting current condition (*SI Appendix*, Table S1).

Pelagic fish covariates were included at the ICES rectangle- and subdivision-level (as pelagic species are highly mobile) (see *SI Appendix*, Figure S1 for the spatial units ICES rectangle and subdivision).

Monthly predictions for sea bottom temperature and sea bottom concentration of dissolved oxygen were extracted at the haul locations from the ocean model NEMO-Nordic-SCOBI (Eilola *et al.*, 2009; Almroth-Rosell *et al.*, 2011; Hordoir *et al.*, 2019) and averaged for October–December (~14, 76, and 10% of the BITS hauls were conducted in October, November, and December, respectively). We also conducted preliminary analysis to determine if oxygen should be modelled with a linear, or a linear threshold effect, as suggested in experimental studies (Chabot and Dutil, 1999; Hrycik *et al.*, 2017). This showed that the model with a linear effect was favoured in terms of Akaike Information Criterion (AIC) (*SI Appendix*, Table S2). Depth raster files were made available by the EMODnet Bathymetry project, <https://www.emodnet.eu/en/bathymetry>, funded by the European Commission Directorate General for Maritime Affairs and Fisheries. Biomass density of *S. entomon* was extracted from a habitat distribution model coupled with modelled hydrographical data from the regional coupled ocean biogeochemical model ERGOM (Gogina *et al.*, 2020; Neumann *et al.*, 2021). The model was trained to the time period 1981–2019 and predicted for the time period 1993–2019 to match the condition data (but note that this prediction is constant over time and therefore better represents *S. entomon* habitats and not temporal variation in biomass density).

All raster-derived covariates (oxygen, temperature, depth, and *S. entomon*) were linked to spatial points using bilinear interpolation (values for a spatial point interpolated from the four nearest raster cells). We used predicted densities of cod and flounder (kg/km²) from GLMMs (described above) as covariates, since not all hauls in the CPUE (density) data could be standardized and joined with the condition data. For the cod and flounder density models that were used to provide covariates for the cod condition model and weights to the body condition predictions, the only fixed effects were year as a factor and a smooth effect of depth. For the cod density models used to evaluate effects of changes in the average depth, oxygen concentration, and temperature, we also included smooth effects of temperature and oxygen as covariates. Biomass of sprat and herring (tonnes) was extracted from the ICES WGBIFS database for the BIAS survey data (<https://www.ices.dk/community/groups/pages/WGBIFS.aspx>).

Following Thorson (2015) and Grüss *et al.* (2020), we rescaled all covariates to have a mean of 0 and a standard deviation of 1. This facilitates comparison between covariates of different units and allows for comparison between the estimated coefficients and the marginal standard deviation of spatial (σ_O) and spatiotemporal (σ_E) variation. We did not conduct any model selection after our *a priori* selection of covariates to avoid statistical issues with inference from stepwise selection (e.g. Whittingham *et al.*, 2006), and because initial analyses suggested the model was not overfit (see also *SI Appendix*, Figure S3 for Pearson correlation coefficients across variables).

Model fitting

For computational efficiency, we fit all models in a “predictive process” modelling framework (Latimer *et al.*, 2009; Anderson and Ward, 2019), where spatial and spatiotemporal

random fields are approximated using a triangulated mesh and the SPDE approximation (Lindgren *et al.*, 2011) (*SI Appendix*, Figures S5 and S17), with the mesh created using the R-package “R-INLA” (Rue *et al.*, 2009). The random effects were estimated at the vertices (“knots”) of this mesh and bilinearly interpolated to the data locations. The locations of the knots were chosen using a *k*-means clustering algorithm, which minimizes the total distance between data points and knots. As the knot random effects are projected to the locations of the observations, more knots generally increase accuracy at the cost of computational time. After initial exploration, we chose 100 knots for the condition model and 200 knots for the density models. We fit the models using “TMB” (Kristensen *et al.*, 2016) via “sdmTMB” (version 0.3.0.9001) (Anderson *et al.*, 2022) with maximum marginal likelihood and the Laplace approximation to integrate over random effects. We assessed convergence by confirming that the maximum absolute gradient with respect to all fixed effects was <0.001 and that the Hessian matrix was positive-definite. Model residuals are shown in the *SI Appendix*, Figures S6–S8 and S18–S19, conditional effects are shown in *SI Appendix*, Figures S13 and S23, and spatial and spatiotemporal random effects are shown in *SI Appendix*, Figures S9 and S10 and S20 and S21. We used packages in the “tidyverse” (Wickham *et al.*, 2019) for data processing and plotting.

Spatiotemporal predictions

We predicted body condition and biomass density of cod onto a 4×4 km prediction grid with covariates to visualize spatiotemporal variation and to calculate random-field model-based indices of condition and relative biomass (Shelton *et al.*, 2014; Thorson *et al.*, 2015a). Annual condition and biomass indices were calculated from 500 draws from the joint precision matrix and model predictions on the grid. Only grid cells with depths between 10 and 110 m were included in these analyses to use only the depths covered by the survey. Predicted condition in each grid cell was weighted with the predicted biomass density of cod in the same grid cell to account for the heterogeneous and temporally varying distribution of biomass in the domain (*SI Appendix*, Figure S4) (Grüss *et al.*, 2020; Indivero *et al.*, 2023). The final annual condition index was acquired by dividing the index by the sum of weights (cod biomass densities) by year. To illustrate the effects of biotic and abiotic covariates on the condition trends over time, we repeated the index calculation based on grid-level condition predicted with the year omitted (set to the initial year, 1993).

Results

The condition model revealed a mean decline in the spatiotemporal biomass-weighted Le Cren condition index of 15% [12%, 19%] from ~ 1.14 [1.1, 1.20] to 0.97 [0.96, 0.98], between 1993 and 2019 (the decline levelled off around 2008) (Figure 1a). The values are medians of 500 draws from the joint precision matrix, and values in brackets are in 2.5 and 97.5% quantiles. The year effect is important for the decline in condition index over time; the index based on predictions only including biotic and abiotic covariates over space and time (omitting the year-specific intercepts) shows a very weak decline initially, only to increase again to levels in the early 1990s (Figure 1a). The condition factor declined in synchrony across subdivisions and in space (*SI Appendix*, Figure S12), but the condition index plateaued at a slightly higher value in

subdivision 24 (Figure 1b). There was in general high agreement between the simple empirical mean condition and the spatiotemporally standardized and biomass-weighted (as well as unweighted) condition index, but in some years the empirical mean was outside the confidence interval of the model-based index (Figure 1). The spatial predictions from the condition model illustrate the presence of consistent “low spots” of body condition. These largely occur in the deep, low-oxygen areas (see e.g. Figure 2 and Figure 5a–b), creating a horizontal dumbbell shape of low-condition spots in the centre of the study area (Figure 2).

The covariates with the largest positive standardized effect sizes on the condition factor were biomass of sprat at the ICES subdivision level [0.008 (0.002, 0.013)] (values in brackets indicate 95% confidence interval), biomass density of *S. entomon* at the rectangle level [0.007 (0.002, 0.012)], temperature at the haul and rectangle level [0.007 (0.0025, 0.01) and 0.007 (0.0018, 0.011), respectively], and oxygen concentration at haul-level [0.004 (0.001, 0.007)] (Figure 3). The effects of median depth, median oxygen, and herring biomass at the rectangle-level, and flounder and cod biomass density at the haul-level were positive but with confidence intervals overlapping 0. The covariates with the largest negative effects were depth at the haul-level [−0.021 (−0.024, −0.018)], subdivision level biomass of herring [−0.005 (−0.01, −0.001)], and biomass of sprat at the ICES rectangle level [−0.04 (−0.006, −0.001)]. Haul-level biomass density of *S. entomon* and rectangle-level median biomass density of cod and flounder were also negatively associated with condition, but with confidence intervals overlapping 0. See also *SI Appendix*, Figure S13 for conditional effects plots of selected variables.

The effect sizes of fixed effects were several times smaller than the magnitude of latent spatiotemporal and spatial variation (Figure 3). The average random effect magnitude was 10 times larger than the average magnitude of individual fixed effects (excluding the year effects) (Figure 3). To address the collective explanatory power of many but small individual fixed effects, we used the approach proposed in Nakagawa and Schielzeth (2013) to calculate marginal R^2 for fixed and random effects. We found that fixed effects had a marginal R^2 of 0.14, while random effects had a marginal R^2 of 0.22 (0.07 for spatial random effects and 0.15 for spatiotemporal random effects). When omitting the fixed year effects, the marginal R^2 for the fixed effects declined to 0.043, and the ratio of R^2 for spatial and spatiotemporal random effects to biotic and abiotic covariates was 5.7 (marginal random R^2 was adjusted to 0.24).

We conducted several sensitivity analyses with respect to the fixed effects. First, we refit the condition model to different parts of the data. The different models were only cod above 30 cm, only cod below 30 cm, omitting subdivision 24 [the mixing zone with western Baltic cod (Mion *et al.*, 2022)], and including only grid-points with cod densities above a certain threshold when calculating median variables across the ICES rectangle. We also explored alternative ways to define the raster-derived large-scale variables. Specifically, instead of using the rectangle averages, we aggregated the raster file to resolutions approximate to the area of an ICES rectangle and then extracted the aggregated value with bilinear interpolation. We also explored different lags for the abiotic covariates (*SI Appendix*, Table S1; Figure S16). However, across all additional models, model coefficients were similar and so was

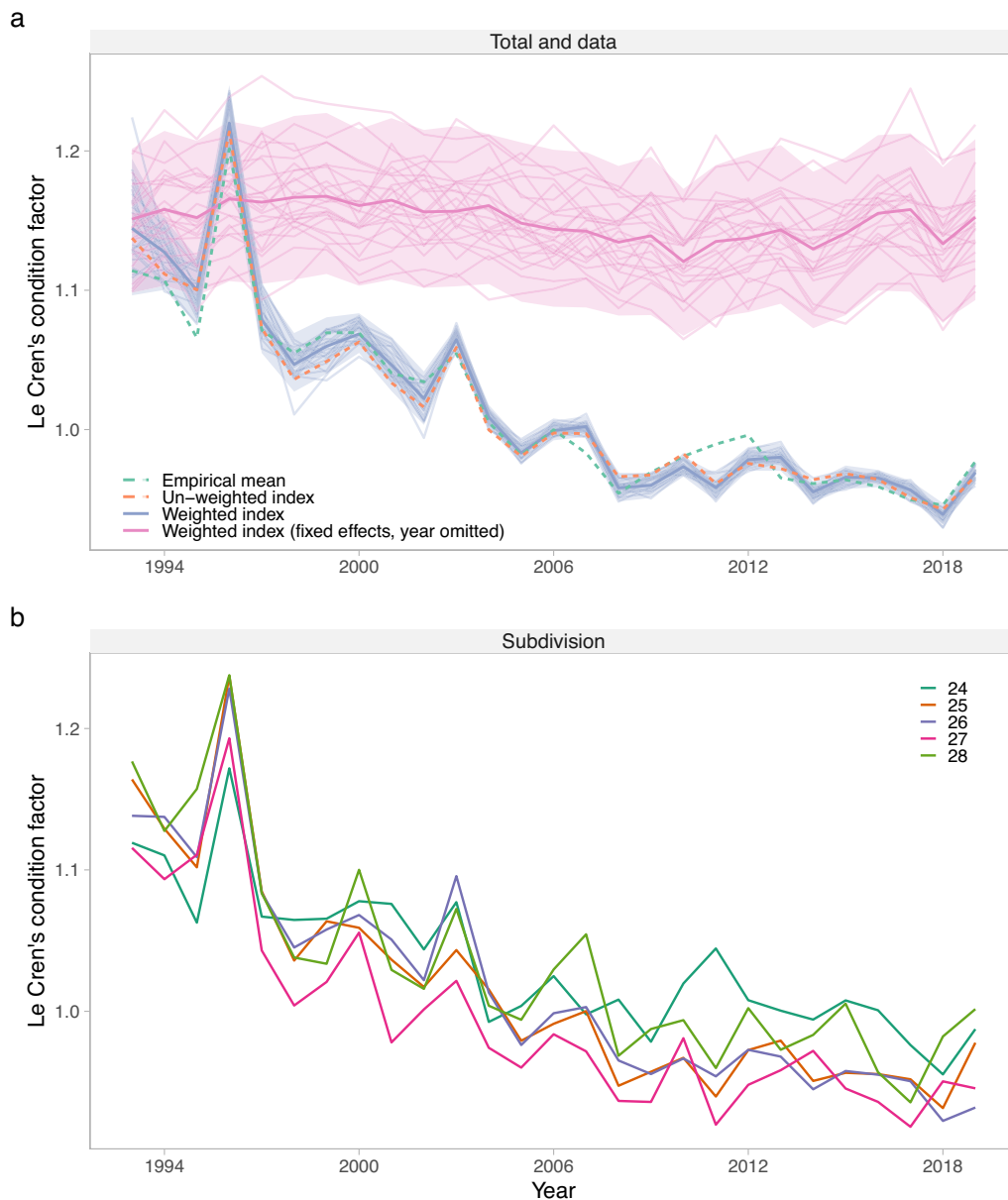


Figure 1. Trends in Le Cren's condition factor between 1993 and 2019 in the Baltic Sea. In panel (a), the empirical mean (green, dotted) is depicted with the spatiotemporal model-predicted unweighted index (orange, dotted) and biomass-weighted Le Cren condition index for the full prediction (blue) and the predictions with only biotic and abiotic fixed effects included (i.e. omitting spatial and spatiotemporal random effects and the year-specific intercepts) (pink). Hence, the latter represents the predicted index given only changes in experienced environmental conditions. Model-based indices were acquired by simulating 500 draws from the joint precision matrix and predicting on a grid with spatially varying covariates set to their true values. ICES rectangles with missing pelagic data were given the subdivision median when predicting but not fitting, see *SI Appendix*, Figure S27. Solid lines depict the mean, the shaded area is the 95% confidence interval and single, thin lines are example draws ($n = 25$) from the joint precision matrix. In panel (b), the index (from the full prediction) is split by ICES subdivision (indicated by colour).

the ratio of spatiotemporal variation and coefficients (*SI Appendix*, Figures S14 and S15).

The median depth and oxygen experienced by cod (depth and oxygen weighted by the predicted biomass density of cod at location, respectively, Figure 4c) got deeper and declined, respectively, throughout the time period (Figure 5). However, the population again occupied slightly shallower waters in the last 3 years of the time series (Figure 5d; see *SI Appendix*, Figure S25 for results split by subdivision). The trends in experienced oxygen were steeper than the average oxygen in the environment at depths corresponding to the interquartile range of cod (Figure 5b–e). The average oxygen concentra-

tion in the environment declined by ~ 0.5 ml/l between 1993 and 2019, while the biomass-weighted oxygen concentration declined more steadily (~ 1 ml/l between 1993 and 2019) (*SI Appendix*, Figure S23 for estimates split by subdivision). The lower quartile of weighted oxygen plateaued around the year 2010. However, while the biomass-weighted oxygen concentration declined between 1993 and 2019 (Figure 5e), the corresponding effect on condition given the effect size of oxygen at the haul was small (*SI Appendix*, Figure S13). The standardized effect size for oxygen (haul-level) of 0.004 means that for each unit increase in the variable (i.e. 1 standard deviation or 1.8 ml/l), the Le Cren condition factor increases by 0.4%. This

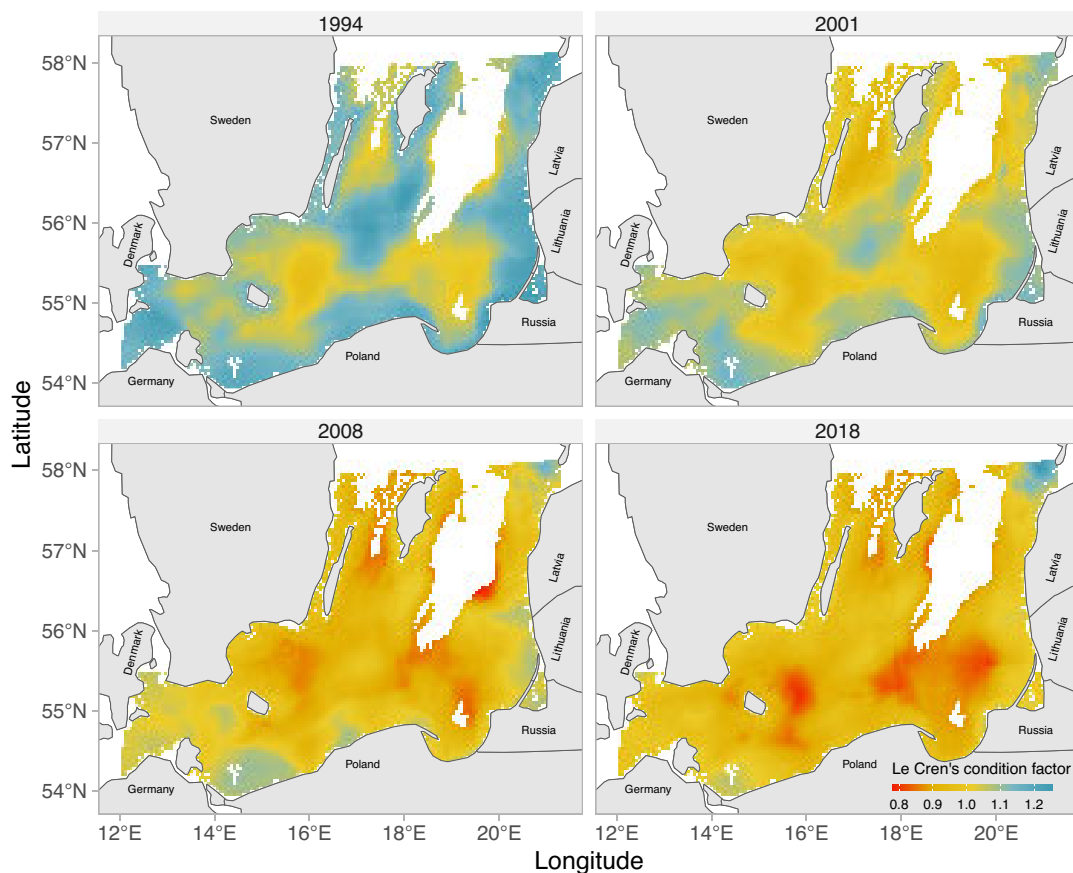


Figure 2. Predicted Le Cren's condition factor with spatially varying covariates set to their true values (ICES rectangles with missing pelagic data were given the subdivision mean, see *SI Appendix*, Figure S27). Included in the plot are years 1994, 2001, 2008, and 2018. Only grid cells with depths between 10 and 110 m are included in the plot. For all years in the series, see *SI Appendix*, Figure S11.

can be compared to the 1 ml/l decline in the experienced oxygen concentration and the 15% decline in the condition factor between 1993 and 2019.

Discussion

The body condition of fish depends on previous energy accumulation and is therefore largely shaped by the quality of the habitat the fish has occupied. By using a spatially explicit condition model, we can link the condition of eastern Baltic cod to covariates at different ecologically relevant spatial scales. Our model reveals that the Le Cren condition factor declined on average by 15% in 1993–2019, with most of this decline occurring in 1993–2008. Moreover, while there are persistent low-spots of body condition (in the deep and low-oxygen areas), the condition declined in the whole area, which suggests that there are drivers acting on large spatial scales. We identify shifts in the spatiotemporal distribution of cod that could have contributed to a decline in cod condition [deeper areas with less oxygen, as in also Casini *et al.* (2021)]. However, effect sizes of single covariates were overall small, and latent spatial and spatiotemporal variation was several times larger in magnitude and explained more variation in condition, a pattern also found in California's Current groundfishes (Thorson, 2015). The magnitude of spatial and spatiotemporal variation suggests that other factors, not explicitly included in our analyses, may have also played an important role in the decline of condition.

Previous studies have suggested both direct (Limburg and Casini, 2019; Brander, 2020) and indirect (Brander, 2020, 2022; Neuenfeldt *et al.*, 2020; Orio *et al.*, 2020) effects of oxygen as a cause for the declining body condition of cod in the past three decades. Direct effects here refer to mild hypoxia reducing the appetite and food consumption (Chabot and Dutil, 1999) and, by extension, also their condition, as their ability to accumulate energy reserves declines. Indirect effects refer to increased competition for benthic prey, as both habitat area and quality are reduced with de-oxygenation. We found that Baltic cod experienced oxygen concentrations at around 7.3 [6–7.6] in 1993 (interquartile range in brackets) ml/l (biomass-weighted median) and are currently (in 2019) experiencing oxygen concentrations at around 6.3 [4.8–7.3] ml/l. In subdivision 25 (the core area of cod, currently), we estimate it to be around 6.4 [4.9–7.3] ml/l between the years 2015 and 2019 (*SI Appendix*, Figure S24). This is higher than recent estimates of an average oxygen concentration of 4–4.5 ml/l, based on oxygen levels at the mean depth of the cod population in recent years (Brander, 2020; Casini *et al.*, 2021).

One reason for the difference in our estimate compared to previous studies is because instead of calculating average oxygen at the mean depth of cod, we weighted the sea bottom oxygen in the environment (from the ocean model NEMO-Nordic-SCOBI) by the predicted densities from the cod density model. This approach overcomes the issue that oxygen concentrations span a large range for any given depth and avoids the assumption that cod depth occupancy is in-

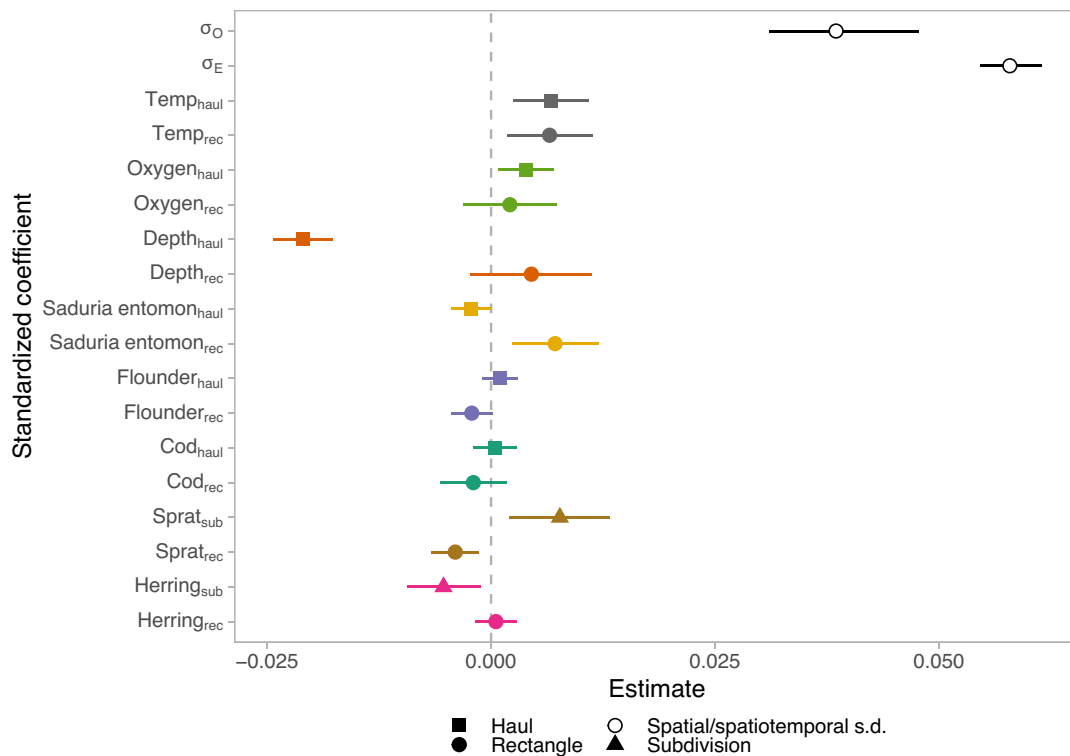


Figure 3. Mean and 95% confidence interval of standardized coefficients (effect sizes) for covariates and spatial and spatiotemporal standard deviation (σ_O and σ_E , respectively) in the condition model. The subscript haul refers to covariates estimated at the location of the haul, rec refers to covariates at the ICES statistical rectangle, and sub refers to covariates over ICES subdivisions (*SI Appendix*, Figure S1). Colours indicate covariate-groups, and shapes indicate scale.

dependent of oxygen concentration. Our finding that trends in weighted and unweighted oxygen differ suggests that it is important to account for species' heterogeneous distribution. This is evident in subdivisions 25 and 27. In subdivision 25, the oxygen trends in the environment have been stable since 2005, as in Svedäng *et al.* (2022), but the experienced oxygen by cod continued to decline. In subdivision 27, the pattern is the opposite with the weighted median being more stable over time than the unweighted mean (*SI Appendix*, Figure S24). Another reason for differences between previous estimates of experienced oxygen could be due to different oxygen models being used. For example, the model developed by Lehmann *et al.* (2002, 2014) (the “GEOMAR” model) and used in Casini *et al.* (2021) and Orio *et al.* (2019), results in, on average, 0.5–1 ml/l lower weighted oxygen concentrations, but also in a less steep decline than the NEMO-Nordic-SCOB model between 1993 and 2016 in subdivision 25 (*SI Appendix*, Figure S28). Also, the unweighted estimates differ ~0.5–1 ml/l between the models at depths between 29 and 61 m. Although explaining the differences between the models is outside the scope of this paper, care should be taken when interpreting absolute values of oxygen concentrations from models.

In an experiment by Chabot and Dutil (1999), 5 ml/l (converted from 73% O₂ saturation at 10°C, 28‰ salinity, and 1013.25 hPa) was estimated to be a critical value, below which negative effects on cod growth and condition were observed. This value is higher than a meta-analytic threshold estimated across fishes of 3.15 ml/l, below which negative effects on fish growth occur (Hryciak *et al.*, 2017). However, despite our data spanning oxygen levels above and below these values, we do

not find support for a threshold in the relationship between condition and oxygen. This is in contrast to what was found in Casini *et al.* (2021) for large cod (small cod showed instead a linear relationship between experienced oxygen and population-level condition). That oxygen is positively associated with condition is in line with both Limburg and Casini (2019) and Casini *et al.* (2021), despite differences in methodological approaches. However, we can only speculate if the positive association is due to higher oxygen being correlated with richer habitats that feature higher food availability, if there are direct physiological impacts at a higher threshold in the wild, or if behavioural responses (e.g. movement between high and low oxygen areas) essentially remove any measurable thresholds in natural systems.

An indirect effect of declining oxygen on condition is the potential amplification of intra- and interspecific competition with flounder for shared benthic prey species, such as the isopod *S. entomon*, due to habitat contraction of cod caused by the expansion of “dead zones” (Casini *et al.*, 2016a, 2021; Orio *et al.*, 2019; Haase *et al.*, 2020). To address the potential effects of changes in intra- and inter-specific competition, we used predicted density of flounder and cod at the haul- and at the ICES rectangle-level, as well as *S. entomon* densities as covariates. We did not detect a negative effect of cod density on cod condition, in contrast to previous studies that suggested density-dependent effects on growth (Svedäng and Hornborg, 2014). Flounder density was also not clearly linked to condition at any scale; however, biomass density is not a direct measure of competition—areas with higher densities of cod and flounder could simply also have more food. It could also be because the biomass of both cod and flounder has been

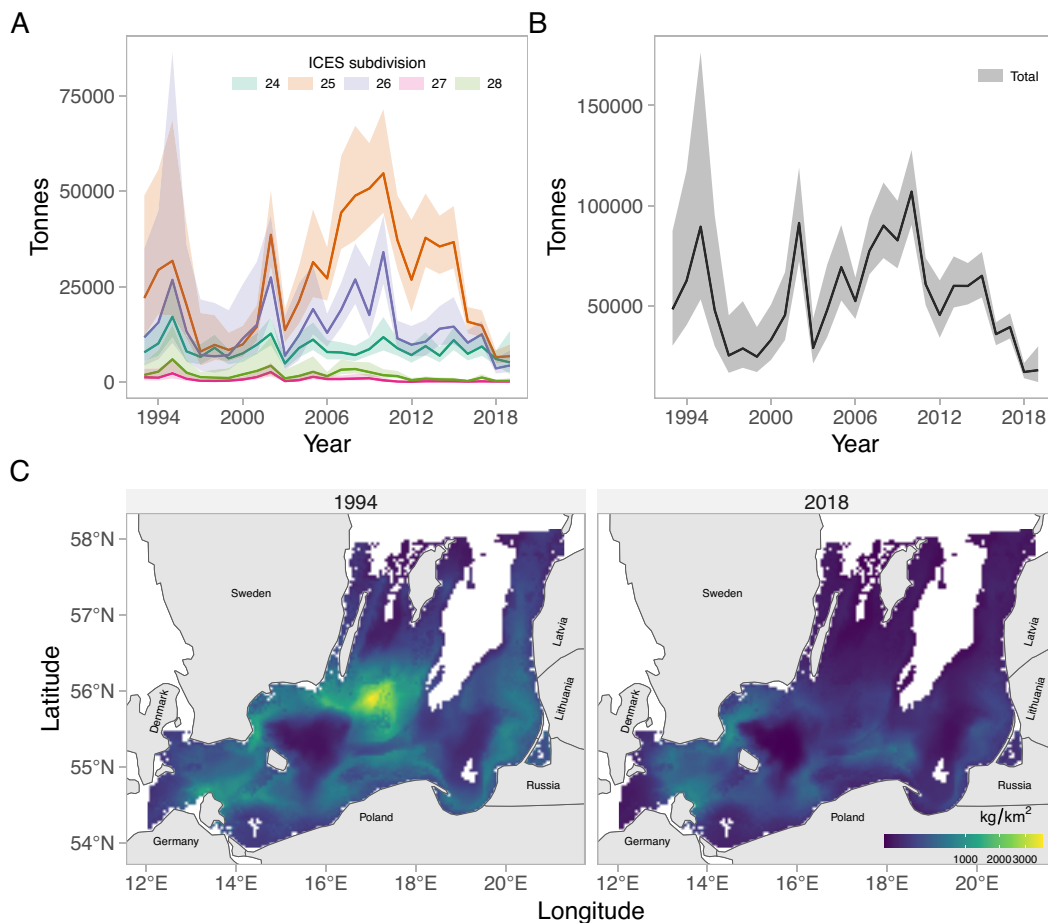


Figure 4. Biomass index from the spatiotemporal density model by ICES subdivision (a) and total across all subdivisions (b). Panel (c) depicts predicted biomass density (kg/km^2) in select years (1994 and 2018). For all years in the series, see *SI Appendix*, Figure S22. Only grid cells with depths between 10 and 110 m are included in the plot.

at relatively low levels during the past three decades from a historical perspective (Tomczak *et al.*, 2022). We do find statistically clear positive effects of *S. entomon* biomass density on condition at the rectangle level. This is interesting because Neuenfeldt *et al.* (2020) found that cod had more *S. entomon* in stomachs in the years 1963–1988 compared to 1994–2014 (but note that the time period 1963–1988 contains years with both low and high body growth and condition in cod) (Casini *et al.*, 2016a; Mion *et al.*, 2021). Unfortunately, we are not able to resolve temporal trends in *S. entomon* over the spatial domain. However, Svedäng *et al.* (2022) recently showed that benthic food availability has not changed dramatically over the time period in the southern Baltic Sea. Therefore, more studies are needed to determine why cod seem to feed less on *S. entomon*, if it is related to competition or shifts in distribution, and how diets rich in *S. entomon* are linked to condition.

A reduced availability of sprat (either changes in their size-distribution or distribution and spatial overlap) has also been linked to poor growth and condition at the population level (Gårdmark *et al.*, 2015; Casini *et al.*, 2016a; Neuenfeldt *et al.*, 2020). In our study, using spatially resolved data, we also found positive effects of sprat biomass on cod condition at the ICES subdivision level (but a negative association on finer scales, possibly because it is too fine a scale for a pelagic and mobile species). The biomass of sprat generally declined from the levels in the early 90s, and this decline is more ac-

centuated in the northern subdivisions analysed, where cod are relatively scarce (*SI Appendix*, Figures S26 and S27). In the main distribution area of cod (subdivisions 24–26), sprat biomass declined from 1993 until around 2010 (where condition plateaued at low values), but after that it increased again to levels close to those in the early 2000s. However, condition did not, and future analyses should therefore further investigate the link between the biomass of pelagic fish and the condition of cod, possibly accounting for condition and size-structure of pelagic species.

Although some were statistically significant, environmental covaraites explained little variation in condition, compared to previous studies using yearly population-level averages of body condition as the response variable (e.g. Casini *et al.*, 2016a). A few, non-mutually exclusive, explanations could be hypothesized for this. The use of data with high spatial resolution allows us to use covariates at different scales and with larger contrasts, but it also necessitates accounting for autocorrelation (which we do by including spatial and spatiotemporal latent variables), else a false sense of confidence could be introduced. Such latent variables can affect fixed effect estimates under some conditions (Hodges and Reich, 2010). Another potential explanation is that predictor variables could have non-linear effects on condition instead of linear effects as we assume. However, supplementary analysis showed that, for example, oxygen was not a more parsimonious predictor when

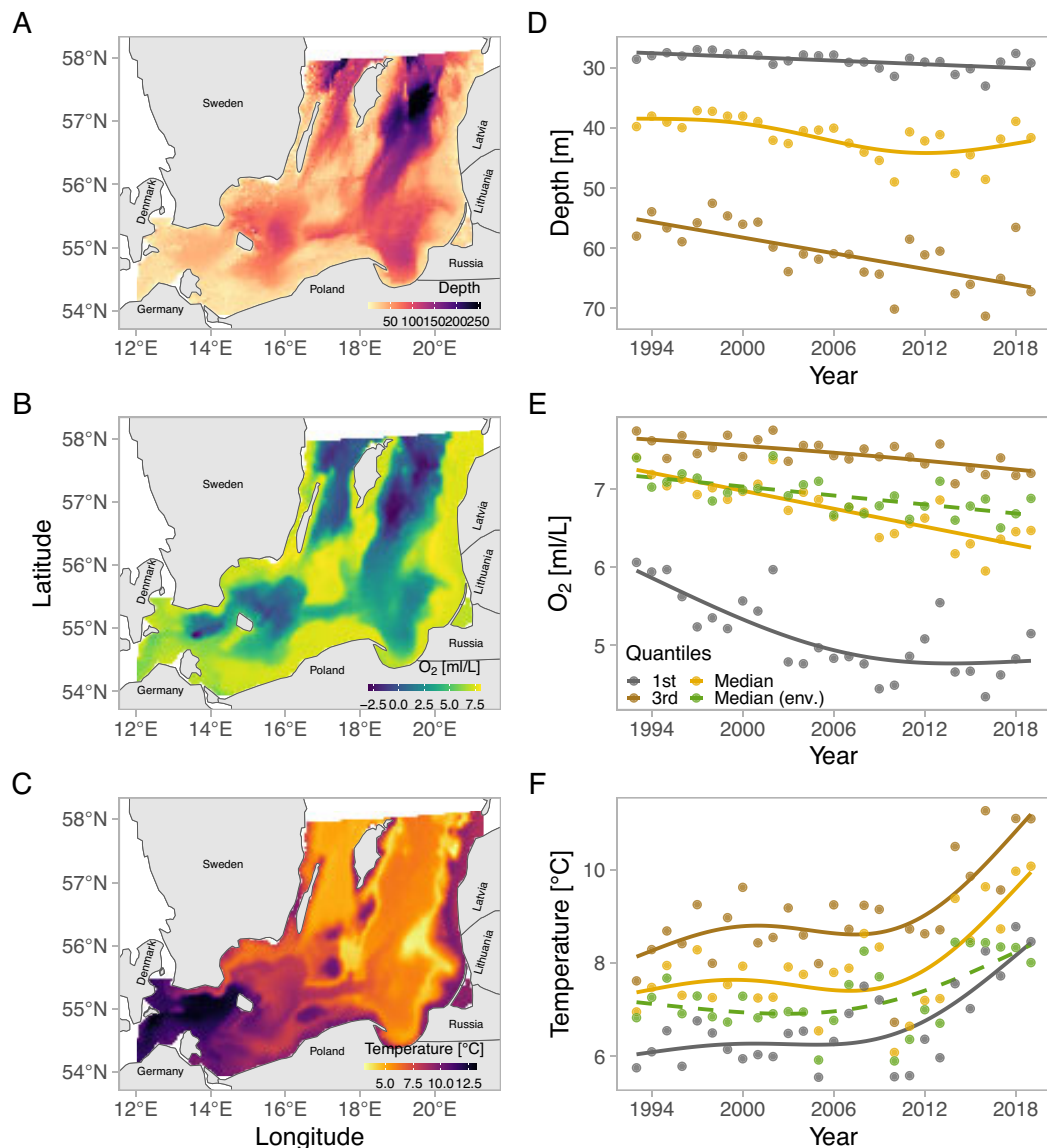


Figure 5. Bathymetry (a), oxygen concentration (b), and temperature (c) (b–c exemplified using the year 2006) in the study area. Panels (d–f) illustrate depth, oxygen, and temperature, respectively, weighted by predicted cod density. Colours indicate biomass-weighted quantiles (first quartile, median, and third quartile), as well as the unweighted median (green dashed line) at depths corresponding to the average interquartile range (29–61 m) for environmental variables. Lines depict generalized additive model fits (basis dimension $k = 4$).

modelled as a breakpoint function. We also assume that effects are constant over time, while in reality they could be time-varying. As an example, liver parasites are numerous now that cod are in poor condition, but likely did not cause the decline as cod in good condition are not as susceptible to parasite infection (Ryberg *et al.*, 2020). Colinearity between predictors could also make single effects unreliable; however, the predicted condition index over time with all covariates included still shows little ability to capture the decline in condition over time. Hence, in our view, mainly two non-mutually exclusive explanations remain: the chosen variables have a small effect on condition, or the variables have an effect, but our covariates do not capture that. The latter could be due to condition being a trait that is shaped over a long time period, while it gets progressively more difficult to match the experienced environment of cod the further back in time one goes because Baltic cod are partly mobile species with large individual variation in

movement behaviour (Hüssy *et al.*, 2020). To further increase our understanding of how the environment shapes spatiotemporal variation in body condition, we suggest that analysis of condition data from surveys conducted with low temporal resolution should be complemented with tagging studies [as suggested by Thorson (2015)] or using “life-time recorders” such as otoliths as done in Limburg and Casini (Limburg and Casini, 2019).

In conclusion, the low explanatory and predictive power of single covariates and the similar biomass-weighted average condition estimated across basins (subdivisions) despite differences in environmental conditions, analysed for the first time in a common framework, suggest that multiple factors are responsible for the observed spatiotemporal changes in cod condition during the past 26 years. The synchrony in temporal trends of condition across basins also suggests that factors acting on large spatial scales have been involved. The

fact that the condition of both herring and sprat also started to decline in the late 1980s and early 1990s (Casini *et al.*, 2011) suggests there could be ecosystem-level drivers, possibly related to productivity. Moreover, in line with Thorson *et al.* (2017), this study shows that it is important to consider the variance explained by covariates for understanding how ecosystem changes and management interventions (Bryhn *et al.*, 2022) that aim to improve habitat quality may affect the productivity of fish stocks via condition. Lastly, since overall stock productivity—of which body condition is a critical component—is so low that the stock is not predicted to grow even in the absence of fishing mortality (ICES, 2021a), it is crucial to gain a deeper understanding of both the past and current drivers of the condition of eastern Baltic cod.

Acknowledgements

We are very grateful for help from Alessandro Orio with standardizing survey data used in the density models, Federico Maioli for help with modelling and data wrangling, Hagen Radtke and Ivan Kuznetsov for assistance in acquiring predictions of *S. entomon* densities, Martin Hansson, Liu Ye and Elin Almroth Rosell at SMHI for assistance with environmental data, and Olavi Kaljuste for providing pelagic data. We also thank three anonymous reviewers and Robyn Forrest for feedback that greatly improved the manuscript. Lastly, we thank the staff involved in the scientific sampling and analysis of biological data.

Supplementary data

Supplementary material is available at the ICESJMS online version of the manuscript.

Funding

The study was financed by the Swedish Research Council Formas (grant no. 2018-00775 to Michele Casini). Mayya Gogina was supported by grant number 03F0848A (DAM pilot mission project MGF Baltic Sea funded by the German Federal Ministry of Education and Research).

Author contributions

All authors contributed to the manuscript. Specifically, M.C. coordinated the study, M.L. prepared the raw data, M.G. provided *S. entomon* data, M.L. led the design and conducted the statistical analyses with critical contribution from S.C.A and input from M.C. and M.L. wrote the first draft. All authors contributed to revisions and gave final approval for publication.

Data and code availability

All code and data to reproduce the results are available on GitHub (<https://github.com/maxlindmark/cod-condition>), and have been deposited on Zenodo (<https://doi.org/10.5281/zenodo.7904131>).

Conflict of interest

The authors declare that they have no conflict of interest.

References

- Almroth-Rosell, E., Eilola, K., Hordoir, R., Meier, H. E. M., and Hall, P. O. J. 2011. Transport of fresh and resuspended particulate organic material in the Baltic Sea—a model study. *Journal of Marine Systems*, 87: 1–12.
- Anderson, S. C., Keppel, E. A., and Edwards, A. M. 2019. A reproducible data synopsis for over 100 species of British Columbia groundfish. DFO Can. Sci. Advis. Sec. Res. Doc. 2019/041. DFO Can. Sci. Advis. Sec. Res. Doc. 2019/041. www.dfo-mpo.gc.ca/csas-sccs/Publications/ResDocs-DocRech/2019/2019_041-eng.html (last accessed March 31, 2021).
- Anderson, S. C., and Ward, E. J. 2019. Black swans in space: modeling spatiotemporal processes with extremes. *Ecology*, 100: e02403.
- Anderson, S. C., Ward, E. J., English, P. A., and Barnett, L. A. K. 2022. sdmTMB: an R package for fast, flexible, and user-friendly generalized linear mixed effects models with spatial and spatiotemporal random fields, bioRxiv 2022.03.24.485545. <https://doi.org/10.1101/2022.03.24.485545> (last accessed 27 March 2023).
- Aro, E. 1989. A review of fish migration patterns in the Baltic. *Rap. Proc.-verb. Re. Cons. Int. Explor. Mer*, 190: 72–96.
- Belkin, I. M. 2009. Rapid warming of large marine ecosystems. *Progress in Oceanography*, 81: 207–213.
- Bolger, T., and Connolly, P. L. 1989. The selection of suitable indices for the measurement and analysis of fish condition. *Journal of Fish Biology*, 34: 171–182.
- Brander, K. 2020. Reduced growth in Baltic Sea cod may be due to mild hypoxia. *ICES Journal of Marine Science*, 77: 2003–2005.
- Brander, K. 2022. Support for the hypothesis that growth of eastern Baltic cod is affected by mild hypoxia. A comment on Svedäng *et al.* (2022). *ICES Journal of Marine Science*, 79: fsac070.
- Breitburg, D. 2002. Effects of hypoxia, and the balance between hypoxia and enrichment, on coastal fishes and fisheries. *Estuaries*, 25: 767–781.
- Bryhn, A. C., Bergek, S., Bergström, U., Casini, M., Dahlgren, E., Ek, C., Hjelm, J. *et al.* 2022. Which factors can affect the productivity and dynamics of cod stocks in the Baltic Sea, Kattegat and Skagerrak? *Ocean & Coastal Management*, 223: 106154.
- Cardinale, M., and Arrhenius, F. 2000. Decreasing weight-at-age of Atlantic herring (*Clupea harengus*) from the Baltic Sea between 1986 and 1996: a statistical analysis. *ICES Journal of Marine Science*, 57: 882–893.
- Carstensen, J., Andersen, J. H., Gustafsson, B. G., and Conley, D. J. 2014. Deoxygenation of the Baltic Sea during the last century. *Proceedings of the National Academy of Sciences*, 111: 5628–5633.
- Casini, M., Cardinale, M., and Hjelm, J. 2006. Inter-annual variation in herring, *Clupea harengus*, and sprat, *Sprattus sprattus*, condition in the central Baltic Sea: what gives the tune? *Oikos*, 112: 638–650.
- Casini, M., Kornilovs, G., Cardinale, M., Möllmann, C., Grygiel, W., Jonsson, P., Raid, T. *et al.* 2011. Spatial and temporal density dependence regulates the condition of central Baltic Sea clupeids: compelling evidence using an extensive international acoustic survey. *Population Ecology*, 53: 511–523.
- Casini, M., Käll, F., Hansson, M., Plikshs, M., Baranova, T., Karlsson, O., Lundström, K. *et al.* 2016a. Hypoxic areas, density-dependence and food limitation drive the body condition of a heavily exploited marine fish predator. *Royal Society Open Science*, 3: 160416.
- Casini, M., Eero, M., Carlshamre, S., and Lövgren, J. 2016b. Using alternative biological information in stock assessment: condition-corrected natural mortality of Eastern Baltic cod. *ICES Journal of Marine Science*, 73: 2625–2631.
- Casini, M., Hansson, M., Orio, A., and Limburg, K. 2021. Changes in population depth distribution and oxygen stratification are involved in the current low condition of the eastern Baltic Sea cod (*Gadus morhua*). *Biogeosciences*, 18: 1321–1331.
- Chabot, D., and Dutil, J.-D. 1999. Reduced growth of Atlantic cod in non-lethal hypoxic conditions. *Journal of Fish Biology*, 55: 472–491.
- Cressie, N.A.C., and Wikle, C. K. 2011. *Statistics for Spatio-Temporal Data*. Wiley, Hoboken, N.J.

- Cui, Y., and Wootton, R. J. 1988. Bioenergetics of growth of a cyprinid, *Phoxinus phoxinus*: the effect of ration, temperature and body size on food consumption, faecal production and nitrogenous excretion. *Journal of Fish Biology*, 33: 431–443.
- Diaz, R. J. 2001. Overview of hypoxia around the world. *Journal of Environmental Quality*, 30: 275–281.
- Diaz, R. J., and Rosenberg, R. 2008. Spreading dead zones and consequences for marine ecosystems. *Science*, 321: 926–929.
- Dutil, J.-D., and Lambert, Y. 2000. Natural mortality from poor condition in Atlantic cod (*Gadus morhua*). *Canadian Journal of Fisheries and Aquatic Sciences*, 57: 826–836.
- Eero, M., Vinther, M., Haslob, H., Huwer, B., Casini, M., Storr-Paulsen, M., and Köster, F. W. 2012. Spatial management of marine resources can enhance the recovery of predators and avoid local depletion of forage fish. *Conservation Letters*, 5: 486–492.
- Eilola, K., Meier, H. E. M., and Almroth, E. 2009. On the dynamics of oxygen, phosphorus and cyanobacteria in the Baltic Sea; a model study. *Journal of Marine Systems*, 75: 163–184.
- Gårdmark, A., Casini, M., Huss, M., van Leeuwen, A., Hjelm, J., Persson, L., and de Roos, A. M. 2015. Regime shifts in exploited marine food webs: detecting mechanisms underlying alternative stable states using size-structured community dynamics theory. *Philosophical Transactions of the Royal Society B: Biological Sciences*, 370: 20130262.
- Gogina, M., Zettler, M. L., Wählström, I., Andersson, H., Radtke, H., Kuznetsov, I., and MacKenzie, B. R. 2020. A combination of species distribution and ocean-biogeochemical models suggests that climate change overrides eutrophication as the driver of future distributions of a key benthic crustacean in the estuarine ecosystem of the Baltic Sea. *ICES Journal of Marine Science*, 77: 2089–2105.
- Grüss, A., Gao, J., Thorson, J., Rooper, C., Thompson, G., Boldt, J., and Lauth, R. 2020. Estimating synchronous changes in condition and density in eastern Bering Sea fishes. *Marine Ecology Progress Series*, 635: 169–185.
- Haase, K., Orio, A., Pawlak, J., Pachur, M., and Casini, M. 2020. Diet of dominant demersal fish species in the Baltic Sea: is flounder stealing benthic food from cod? *Marine Ecology Progress Series*, 645: 159–170.
- Hislop, J. R. G., Robb, A. P., and Gauld, J. A. 1978. Observations on effects of feeding level on growth and reproduction in haddock, *Melanogrammus aeglefinus* (L.) in captivity. *Journal of Fish Biology*, 13: 85–98.
- Hodges, J. S., and Reich, B. J. 2010. Adding spatially-correlated errors can mess up the fixed effect you love. *The American Statistician*, 64: 325–334.
- Hordoir, R., Axell, L., Höglund, A., Dieterich, C., Fransner, F., Gröger, M., Liu, Y. *et al.* 2019. Nemo-Nordic 1.0: a NEMO-based ocean model for the Baltic and North seas—research and operational applications. *Geoscientific Model Development*, 12: 363–386.
- Hryciuk, A. R., Almeida, L. Z., and Höök, T. O. 2017. Sub-lethal effects on fish provide insight into a biologically-relevant threshold of hypoxia. *Oikos*, 126: 307–317.
- Hüssy, K., Casini, M., Haase, S., Hilvarsson, A., Horbowy, J., Krüger-Johnsen, M., Krumme, U. *et al.* 2020. Tagging Baltic Cod—TABACOD. Eastern Baltic cod: solving the ageing and stock assessment problems with combined state-of-the-art tagging methods. DTU Aqua Report, 368–2020pp. National Institute of Aquatic Resources, Kemitovet, 2800 Kgs.. Lyngby, Denmark.
- ICES. 2021a. Cod (*Gadus morhua*) in subdivisions 24–32, eastern Baltic stock (eastern Baltic Sea). In Report of the ICES Advisory Committee. ICES ADVICE 2021 cod.27.24–32. <https://doi.org/10.17895/ices.advice.7745> (last accessed 9 December 2022).
- ICES. 2021b. Baltic fisheries assessment working group (WGB-FAS). ICES Scientific Reports. <https://doi.org/10.17895/ices.pub.8187> (last accessed 9 December 2022).
- Indivero, J., Essington, T. E., Ianelli, J. N., and Thorson, J. T. 2023. Incorporating distribution shifts and spatio-temporal variation when estimating weight-at-age for stock assessments: a case study involving the Bering Sea pollock (*Gadus chalcogrammus*). *ICES Journal of Marine Science*, 80: 258–271.
- Jørgensen, C., Ernande, B., Fiksen, Ø., and Dieckmann, U. 2006. The logic of skipped spawning in fish. *Canadian Journal of Fisheries and Aquatic Sciences*, 63: 200–211.
- Kristensen, K., Nielsen, A., Berg, C. W., Skaug, H., and Bell, B. M. 2016. TMB: automatic differentiation and laplace approximation. *Journal of Statistical Software*, 70: 1–21.
- Latimer, A. M., Banerjee, S., Sang, H., Mosher, E. S., and Silander, J. A. 2009. Hierarchical models facilitate spatial analysis of large data sets: a case study on invasive plant species in the northeastern United States. *Ecology Letters*, 12: 144–154.
- Le Cren, E. D. 1951. The length-weight relationship and seasonal cycle in gonad weight and condition in the perch (*Perca fluviatilis*). *Journal of Animal Ecology*, 20: 201–219.
- Lehmann, A., Krauss, W., and Hinrichsen, H.-H. 2002. Effects of remote and local atmospheric forcing on circulation and upwelling in the Baltic Sea. *Tellus A*, 54: 299–316.
- Lehmann, A., Hinrichsen, H.-H., Getzlaff, K., and Myrberg, K. 2014. Quantifying the heterogeneity of hypoxic and anoxic areas in the Baltic Sea by a simplified coupled hydrodynamic-oxygen consumption model approach. *Journal of Marine Systems*, 134: 20–28.
- Limburg, K. E., and Casini, M. 2019. Otolith chemistry indicates recent worsened Baltic cod condition is linked to hypoxia exposure. *Biology Letters*, 15: 20190352.
- Lindgren, F., Rue, H., and Lindström, J. 2011. An explicit link between Gaussian fields and Gaussian Markov random fields: the stochastic partial differential equation approach. *Journal of the Royal Statistical Society: Series B (Statistical Methodology)*, 73: 423–498.
- Lloret, J., Shulman, G., and Love, R. M. 2014. Condition and Health Indicators of Exploited Marine Fishes. John Wiley & Sons, Chichester, UK. 247pp.
- Marshall, C. T., and Frank, K. T. 1999. The effect of interannual variation in growth and condition on haddock recruitment. *Canadian Journal of Fisheries and Aquatic Sciences*, 56: 347–355.
- Mion, M., Thorsen, A., Vitale, F., Dierking, J., Herrmann, J. P., Huwer, B., von Dewitz, B. *et al.* 2018. Effect of fish length and nutritional condition on the fecundity of distressed Atlantic cod *Gadus morhua* from the Baltic Sea. *Journal of Fish Biology*, 92: 1016–1034.
- Mion, M., Haase, S., Hemmer-Hansen, J., Hilvarsson, A., Hüssy, K., Krüger-Johnsen, M., Krumme, U. *et al.* 2021. Multidecadal changes in fish growth rates estimated from tagging data: a case study from the Eastern Baltic cod *Gadus morhua*, Gadidae). *Fish and Fisheries*, 22: 413–427.
- Mion, M., Griffiths, C., Bartolino, V., Haase, S., Hilvarsson, A., Hüssy, K., Krüger-Johnsen, M. *et al.* 2022. New perspectives on Eastern Baltic cod movement patterns from historical and contemporary tagging data. *Marine Ecology Progress Series*, 689: 109–126.
- Möllmann, C., Kornilovs, G., Fetter, M., Köster, F. W., and Hinrichsen, H.-H. 2003. The marine copepod, *pseudocalanus elongatus*, as a mediator between climate variability and fisheries in the Central Baltic Sea. *Fisheries Oceanography*, 12: 360–368.
- Morgan, M. J., Rideout, R. M., and Colbourne, E. B. 2010. Impact of environmental temperature on Atlantic cod *Gadus morhua* energy allocation to growth, condition and reproduction. *Marine Ecology Progress Series*, 404: 185–195.
- Nakagawa, S., and Schielzeth, H. 2013. A general and simple method for obtaining R² from generalized linear mixed-effects models. *Methods in Ecology and Evolution*, 4: 133–142.
- Nash, R., Valencia, A., and Geffen, A. 2006. The origin of fulton's condition factor: setting the record straight. *Fisheries*, 31: 236–238.
- Neuenfeldt, S., Bartolino, V., Orio, A., Andersen, K. H., Andersen, N. G., Niiranen, S., Bergström, U. *et al.* 2020. Feeding and growth of Atlantic cod (*Gadus morhua* L.) in the eastern Baltic Sea under environmental change. *ICES Journal of Marine Science*, 77: 624–632.
- Neumann, T., Koponen, S., Attila, J., Brockmann, C., Kallio, K., Kervinen, M., Mazeran, C. *et al.* 2021. Optical model for the Baltic Sea

- with an explicit CDOM state variable: a case study with Model ER-GOM (version 1.2). *Geoscientific Model Development*, 14: 5049–5062.
- Orio, A., Florin, A.-B., Bergström, U., Šics, I., Baranova, T., and Casini, M. 2017. Modelling indices of abundance and size-based indicators of cod and flounder stocks in the Baltic Sea using newly standardized trawl survey data. *ICES Journal of Marine Science*, 74: 1322–1333.
- Orio, A., Bergström, U., Florin, A.-B., Lehmann, A., Šics, I., and Casini, M. 2019. Spatial contraction of demersal fish populations in a large marine ecosystem. *Journal of Biogeography*, 46: 633–645.
- Orio, A., Bergström, U., Florin, A.-B., Šics, I., and Casini, M. 2020. Long-term changes in spatial overlap between interacting cod and flounder in the Baltic Sea. *Hydrobiologia*, 847: 2541–2553.
- Reusch, T. B. H., Dierking, J., Andersson, H. C., Bonsdorff, E., Carstensen, J., Casini, M., Czajkowski, M. *et al.* 2018. The Baltic Sea as a time machine for the future coastal ocean. *Science Advances*, 4. American Association for the Advancement of Science. <https://www.science.org/doi/abs/10.1126/sciadv.aar8195> (last accessed 1 September 2021)..
- Rue, H., Martino, S., and Chopin, N. 2009. Approximate bayesian inference for latent Gaussian models by using integrated nested Laplace approximations. *Journal of the Royal Statistical Society: Series B (Statistical Methodology)*, 71: 319–392.
- Ryberg, M. P., Skov, P. V., Vendramin, N., Buchmann, K., Nielsen, A., and Behrens, J. W. 2020. . <https://academic.oup.com/conphys/article/8/1/coaa093/5909674> (last accessed 13 November 2020)..
- Shelton, A. O., Thorson, J. T., Ward, E. J., and Feist, B. E. 2014. Spatial semiparametric models improve estimates of species abundance and distribution. *Canadian Journal of Fisheries and Aquatic Sciences*, 71: 1655–1666.
- Shono, H. 2008. Application of the Tweedie distribution to zero-catch data in CPUE analysis. *Fisheries Research*, 93: 154–162.
- Svedäng, H., and Hornborg, S. 2014. Selective fishing induces density-dependent growth. *Nature Communications*, 5: 4152.
- Svedäng, H., Savchuk, O., Villnäs, A., Norkko, A., Gustafsson, B. G., Wikström, S. A., and Humborg, C. 2022. Re-thinking the “ecological envelope” of Eastern Baltic cod (*Gadus morhua*): conditions for productivity, reproduction, and feeding over time. *ICES Journal of Marine Science*, 79: fsac017.
- Thorson, J. T. 2015. Spatio-temporal variation in fish condition is not consistently explained by density, temperature, or season for California current groundfishes. *Marine Ecology Progress Series*, 526: 101–112.
- Thorson, J. T., Shelton, A. O., Ward, E. J., and Skaug, H. J. 2015a. Geostatistical delta-generalized linear mixed models improve precision for estimated abundance indices for West Coast groundfishes. *ICES Journal of Marine Science*, 72: 1297–1310.
- Thorson, J. T., Scheuerell, M. D., Shelton, A. O., See, K. E., Skaug, H. J., and Kristensen, K. 2015b. Spatial factor analysis: a new tool for estimating joint species distributions and correlations in species range. *Methods in Ecology and Evolution*, 6: 627–637.
- Thorson, J. T., Ianelli, J. N., and Kotwicki, S. 2017. The relative influence of temperature and size-structure on fish distribution shifts: a case-study on walleye pollock in the Bering Sea. *Fish and Fisheries*, 18: 1073–1084.
- Tomczak, M. T., Müller-Karulis, B., Blenckner, T., Ehrnsten, E., Eero, M., Gustafsson, B., Norkko, A. *et al.* 2022. Reference state, structure, regime shifts, and regulatory drivers in a coastal sea over the last century: the Central Baltic Sea case. *Limnology and Oceanography*, 67: S266–S284.
- Tweedie, M. C. 1984. An index which distinguishes between some important exponential families. In *Statistics: Applications and New Directions: Proc. Indian Statistical Institute Golden Jubilee International Conference*, 579–604pp.
- Whittingham, M. J., Stephens, P. A., Bradbury, R. B., and Freckleton, R. P. 2006. Why do we still use stepwise modelling in ecology and behaviour? *Journal of Animal Ecology*, 75: 1182–1189.
- Wickham, H., Averick, M., Bryan, J., Chang, W., D’Agostino McGowan, L., François, R., Golemund, G. *et al.* 2019. Welcome to the tidyverse: 1686. *Journal of Open Source Software*, 4: 1686.

Handling editor: Henn Ojaveer